Taylor & Francis
Taylor & Francis Group

ORIGINAL RESEARCH

🔓 OPEN ACCESS Check for updates

CD39+ conventional CD4+ T cells with exhaustion traits and cytotoxic potential infiltrate tumors and expand upon CTLA-4 blockade

Sabrina N. Bossio[a,b], Carolina Abrate[a,b,‡], Jimena Tosello Boari[c,‡], Constanza Rodriguez[a,b], Fernando P. Canale[a,b], María C. Ramello[a,b], Valentina Brunotto[a,b], Wilfrid Richer[c], Dario Rocha[d], Christine Sedlik[c], Anne Vincent-Salomon[e], Edith Borcoman[f], Andres Del Castillo[g], Adriana Gruppi[a,b], Elmer Fernandez[d], Eva V. Acosta Rodríguez[a,b], Eliane Piaggio[c,†], and Carolina L. Montes[a,b,†]

[a]Departamento de Bioquímica Clínica, Facultad de Ciencias Químicas, Universidad Nacional de Córdoba, Córdoba, Argentina; [b]Centro de Investigaciones en Bioquímica Clínica e Inmunología (CIBICI-CONICET), Córdoba, Argentina; [c]Institut Curie Research Center, Translational Research Department, INSERM U932, PSL Research University, Paris, France; [d]Centro de Investigación y desarrollo en inmunología y enfermedades infecciosas (CIDIE-CONICET), Argentina; [e]Diagnostic and Theranostic Medicine Division, Institut Curie, PSL Research University, Paris, France; [f]Department of Medical Oncology, Institut Curie, Paris, France; [g]Hospital Rawson, Polo Sanitario, Córdoba, Argentina

ABSTRACT

Conventional CD4+ T (Tconv) lymphocytes play important roles in tumor immunity; however, their contribution to tumor elimination remains poorly understood. Here, we describe a subset of tumor-infiltrating Tconv cells characterized by the expression of CD39. In several mouse cancer models, we observed that CD39+ Tconv cells accumulated in tumors but were absent in lymphoid organs. Compared to tumor CD39− counterparts, CD39+ Tconv cells exhibited a cytotoxic and exhausted signature at the transcriptomic level, confirmed by high protein expression of inhibitory receptors and transcription factors related to the exhaustion. Additionally, CD39+ Tconv cells showed increased production of IFNγ, granzyme B, perforin and CD107a expression, but reduced production of TNF. Around 55% of OVA-specific Tconv from B16-OVA tumor-bearing mice, expressed CD39. *In vivo* CTLA-4 blockade induced the expansion of tumor CD39+ Tconv cells, which maintained their cytotoxic and exhausted features. In breast cancer patients, CD39+ Tconv cells were found in tumors and in metastatic lymph nodes but were less frequent in adjacent non-tumoral mammary tissue and not detected in non-metastatic lymph nodes and blood. Human tumor CD39+ Tconv cells constituted a heterogeneous cell population with features of exhaustion, high expression of inhibitory receptors and CD107a. We found that high CD4 and ENTPD1 (CD39) gene expression in human tumor tissues correlated with a higher overall survival rate in breast cancer patients. Our results identify CD39 as a biomarker of Tconv cells, with characteristics of both exhaustion and cytotoxic potential, and indicate CD39+ Tconv cells as players within the immune response against tumors.

Introduction

The role of CD4+ Tconv cells in controlling or enhancing tumor response is not completed understood. However, antigen-specific Tconv cells accumulate at tumor sites, supporting their involvement in anti-tumor effector functions, in both mouse experimental models and human cancer.[1,2]

Antigen-driven activation of naïve CD4+ T cells leads to their differentiation into effector subsets. Differentiated CD4+ T cells (e.g., Th1, Th2, Th17, and regulatory T cells) impact tumor immunity by influencing other cell types.[3,4] A less described cytotoxic activity has been observed in a subset of CD4+ T cells (cytotoxic CD4+ T cells, CTLs).[5] CD4+ CTLs were identified in murine cancer models as well as in melanoma patients,

where melanoma-specific CD4+ T cells gained cytotoxic activity and eradicated tumors in a MHCII-dependent fashion[6,7].

Within the tumor microenvironment (TME), CD4+ T cell populations have been described with effector, regulatory, and exhaustion features.[8,9] T cell exhaustion was initially described in CD8+ T lymphocytes, in animal models and in patients with cancers or chronic viral infections[10–12]. CD8+ T cell exhaustion is characterized by reduced effector cytokine production and the co-expression of inhibitory receptors (iRs).[12] Exhausted CD8+ T cells display a distinct patter of transcription factors (TFs) such as T-bet, Eomes, Blimp-1, and TOX.[13,14] We recently described that CD39, an ecto-nucleotidase involved in adenosine production, defines cell exhaustion in human and mouse

tumor-infiltrating (T-I) CD8^{+} T cells.[15] In addition, CD39 identifies tumor-reactive CD8^{+} T cells in human solid tumors.[16]

Related to CD4 T cell compartment, it has been demonstrated that T-I PD-1^{high}CD39^{+} Tconv cells from head and neck, ovarian, and cervical cancer patients exhibit features of T cell exhaustion.[17] CD39 also identifies a tumor-specific CD4^{+}Foxp3^{−} T cell population in squamous cell carcinoma patients.[18]

Here, we describe that CD39^{+} Tconv infiltrate tumors from mouse cancer models and breast cancer (BC) patients. Using phenotypic and transcriptional approaches, we demonstrate that CD39^{+} Tconv exhibit features of exhaustion and transcriptional signature of cytotoxic T cells. Together, our findings reinforce the idea that the CD39^{+} Tconv population likely plays a significant role in the immune response against tumors.

Materials and methods

Mouse and human samples

Mice (6–10 weeks) were housed at the animal facility of the CIBICI-CONICET. Animal protocols were approved by the Institutional Animal Care and Use Committee (IACUC) of the CIBICI-CONICET.

Human tumors, juxtatumoral breast tissues (adjacent non-tumoral mammary tissues), and tumor-draining lymph nodes (dLNs) were collected from 49 untreated female BC patients undergoing standard-of-care surgery at the Institut Curie Hospital (France) and the Hospital Rawson (Argentina). The BC patients were untreated prior to surgery and free of chronic infections. Clinical and pathological data of recruited/analyzed BC patients are described in Supplementary Table S1. All protocols were approved by the institutional review boards and all patients signed an informed consent form. dLNs were classified by histology into metastatic or non-metastatic according to the presence of tumor cells, and confirmed by Epcam/CD45 staining using flow cytometry. Blood was sampled from patients of Hospital Rawson. All studies in patients were conducted in accordance with the ethical guidelines of the Declaration of Helsinki.

Tumors and dLNs were disaggregated mechanically and enzymatically with liberase and DNase I (Roche). Peripheral blood mononuclear cells (PBMCs) were isolated by centrifugation over Ficoll-Paque gradients (GE Healthcare).

Cell lines

MC38 and MCA-OVA were kindly provided by Dr. Clothilde Théry. 4T1 and B16F10-OVA cell lines were purchased from ATCC. B16F10-OVA and MC38 were maintained in DMEM (GIBCO). 4T1 and MCA-OVA in RPMI-1640. Media were supplemented with 10% Fetal Bovine Serum (GIBCO), 1 mM L-Glutamine (GIBCO), 25 mmol/L Hepes (Cell Gro), and 40 μg/mL gentamicin sulfate (Richet).

In vivo tumor models

Male C57BL/6 or Foxp3-EGFP reporter mice were inoculated subcutaneously (s.c.) with 1×10^6 B16F10-OVA, 0.5×10^6 MC38, or 0.5×10^6 MCA-OVA cells. Female Balb/c mice were inoculated s.c. with 3×10^4 4T1 cells. Tumors excised at day indicated in each figure were disaggregated mechanically and enzymatically with 2 mg/mL collagenase IV and 50 U/mL DNase I (Roche).

ATP hydrolysis assay

Sorted CD39^{+} Tconv, CD39^{−} Tconv and Treg cells from B16F10-OVA tumor-bearing Foxp3-EGFP mice were incubated with 5 μM of exogenous ATP (Sigma-Aldrich) as previously described.[19] Cell-free medium was then analyzed for residual ATP with ATP bioluminescent assay kit (INVITROGEN). Bioluminescent activity was measured with a Synergy HTX Multi-Mode Reader.

Anti-CTLA-4 blockade

Male C57BL/6 mice were inoculated s.c. with 0.5×10^6 MC38 cells. Tumor-bearing mice were treated with anti-CTLA-4 (BioXCell) ($n = 8$) or control IgG ($n = 8$) (Syrian hamster IgG BioXCell), following the protocol depicted in Figure 4a.

Flow cytometry

Single cell suspensions were stained with monoclonal antibodies against mouse and human antigens. For fluorochromes and clones, refer to Supplementary Table S2. Gating strategies for cellular populations from mouse and human tissues are shown in Supplementary Figure S1.

TFs (intracellular staining) and intracellular cytokine detection cells were performed following protocols previously described.[15,20]

OVA-specific Tconv cells were identified using a BV421-labeled H-2 IAb tetramer specific to OVA[323–339] (HAAHAEINEA) (NIH Tetramer Core Facility). As a control for specific staining, a BV421-labeled H-2 IAb tetramer (PVSKMRMATPLLMQA) was utilized. Percoll-purified TILs were incubated with mouse FcR Blocker, followed by staining with the tetramer or control for 2 h at 37°C. Then, cells were stained with surface and intracellular markers.

Samples were acquired in a BD LSR Fortessa flow cytometer (BD Biosciences) and the data analyzed with FlowJO[TM] software.

Cell sorting and RNA isolation for RNA sequencing

B16F10-OVA tumors from 9 Foxp3-EGFP tumor-bearing mice were processed for RNA sequencing. Tumors were shaped into 3 pools, and purified CD4^{+} T cells were obtained by positive selection with the "EasySep Mouse CD4 Positive Selection II" kit (StemCell Technologies). Then, cells were stained with CD45-AF700, TCRβ-APC-Cy7, CD8-APC, CD4-PE-TexasRed, CD39-PE, CD11b-PE-Cy7, CD19-PE-Cy7, NK1.1-PE-Cy7, F4/80-PE-Cy7, and later with 4',6-dia-midino-2-phenylindole (DAPI) LIVE/DEAD stain. Among the live CD4^{+} T cells (DAPI- CD11b- CD19- NK1.1- F4/80-CD8- CD45+ TCRβ+ CD4+), an equal number of Treg, CD39^{+} Tconv, and CD39^{−} Tconv were sorted with a purity of 98–99%, using a BD FACS ARIA II cell sorter (GFP+,

GFP- CD39+, GFP- CD39-, respectively). Cells were lysed with TCL buffer (Qiagen) with 1% of ß-mercaptoethanol and stored at – 80°C.

RNA was isolated using a Single Cell RNA purification kit (Norgen), including RNase-Free DNase Set (Qiagen) treatment. RNA integrity numbers were evaluated with an Agilent RNA 6000 pico kit. Samples were assessed following the manufacturer's instructions.

RNA sequencing

Reverse transcription and cDNA amplification were performed with the SMART-Seq v4 Ultra Low Input RNA Kit (Takara). Barcoded Illumina-compatible libraries were generated from 5 to 10 ng of DNA of each sample, using the Nextera XTP Preparation Kit (illumina). Libraries were sequenced on an Illumina Novaseq 6000 using 100 bp paired-end mode, 20 million reads per sample.

RNA analysis

FASTQ files were mapped to the ENSEMBL Mouse (GRCm38/mm10) reference using STAR 2.3[21] (STAR, RRID:SCR_004463) and counted by the feature Counts from the RSubread R package. Read count normalization and group comparisons were performed with EdgeR (edgeR, RRID:SCR_012802) and limma R libraries. Genes in which total sum counts per million were > 10 were kept for differential expression analysis. Differential expression between experimental conditions was defined by using the "treat" limma method, using p-value ≤0.05 and fold change ≥ 2. Volcano plots were made with R Version + 3 and imaged by Java Treeview software. Functional analyses were performed with GSEA and the Panther Classification System. GEO Accession ID: GSE21881.

TCGA data

The Cancer Genome Atlas (TCGA)[22] data was downloaded with TCGA assembler.[23] Raw counts and transcripts per million (TPM) were obtained for expression data. Normalization factors for raw count data were calculated by Trimmed Mean of M-values (TMM) with the EdgeR package.[24] Raw count expression data was transformed to $\log_2$ (counts per million + 0.5).

Survival analysis

The expression of PTPRC, CD4, and FOXP3 genes was categorized as "high" or "low" according to the median. Samples with high PTPRC, high CD4, and low FOXP3 expression were selected for analysis. CD39 expression was categorized into "high" or "low" according to a cutpoint defined by maximizing the log-rank statistic of a Kaplan-Meier model for overall survival, using the surv_cutpoint function of the survminer R package.[25]

Statistical analysis

GraphPad Prism 8.0 software was used for statistical analysis. The statistical analysis used with mouse or human samples are indicated in each legend for figure. P values < 0.05 were considered statistically significant. Z-score was estimated as: $(MFI-MFI_{average})/SD$.

Results

CD39$^+$ Tconv cells infiltrate tumors from mouse experimental models

We first explored the presence of CD39-expressing Tconv cells (CD4$^+$FOXP3$^-$) in tumor, spleen, and tumor-draining lymph nodes (dLNs) from B16F10-OVA tumor-bearing mice. On day 17 post injection (p.i.), we observed that around 50% of T-I Tconv expressed CD39. In contrast to tumor, CD39$^+$ Tconv were nearly absent in dLNs and spleen (Figure 1a). Low frequencies of this cell subset were detected in dLNs (1.63 ± 0.23) and spleen (4.18 ± 1.08) from tumor-free mice. As observed in the B16F10-OVA model, Tconv from mice bearing MCA-OVA, MC38 or 4T1 tumors also showed a high frequency of CD39$^+$ cells (Supplementary Fig. S2 A-C), while, in lymphoid organs, CD39$^+$ Tconv cells were present at significantly lower frequencies than in tumors. This indicates that CD39 expression on Tconv cells is associated with the TME, and that CD39 expression in T-I Tconv is a common feature across tumors of different histological origin.

Considering that CD39 is highly expressed by Treg, we compared CD39 expression in T-I Tconv and Treg from B16F10-OVA tumor-bearing mice. We observed that CD39 expression, determined as Mean Fluorescence Intensity (MFI), in CD39$^+$ Tconv was similar to that observed in CD39$^+$ Treg (Figure 1b). We also observed similar frequencies of CD39$^+$ Tconv and Treg among T-I CD4$^+$ T cells (Figure 1c). In addition, we found that CD39$^+$ Tconv cells, demonstrated higher ability to hydrolyze extracellular ATP (eATP) compared to CD39$^-$ Tconv cells. Moreover, the ability was comparable to that observed by Treg (Figure 1d).

A kinetic study in B16F10-OVA tumors showed that the frequency of CD39$^+$ Tconv increased with tumor progression. Indeed, the percentage of T-I CD39$^+$ Tconv was significantly higher at day 24 p.i than at day 10 p.i. (Figure 1e). In addition, we detected a linear correlation between the frequency of T-I CD39$^+$ Tconv cells and tumor volume (Figure 1f).

We further characterized the activation/differentiation phenotype of T-I CD39$^+$ Tconv and found that most of these cells exhibited an effector memory (EM) phenotype (CD62L$^-$CD44$^+$). We found naïve cells (CD62L$^+$CD44$^-$) only among CD39$^-$ Tconv (Figure 1g). These results suggest that, within the TME, Tconv cells including CD39$^+$ T cells, have probably undergone antigenic stimulation.

CD73 is an enzyme that works in cooperation with CD39 in converting eATP to adenosine. We detected comparable frequencies of CD73$^+$ cells both when comparing CD39$^+$ Tconv and CD39$^+$ Treg and when comparing CD39$^+$ and CD39$^-$ Tconv cells. We did not find any significant difference in the CD73 expression (MFI) among CD39$^+$ Treg and CD39$^+$ Tconv cells (Figure 1h).
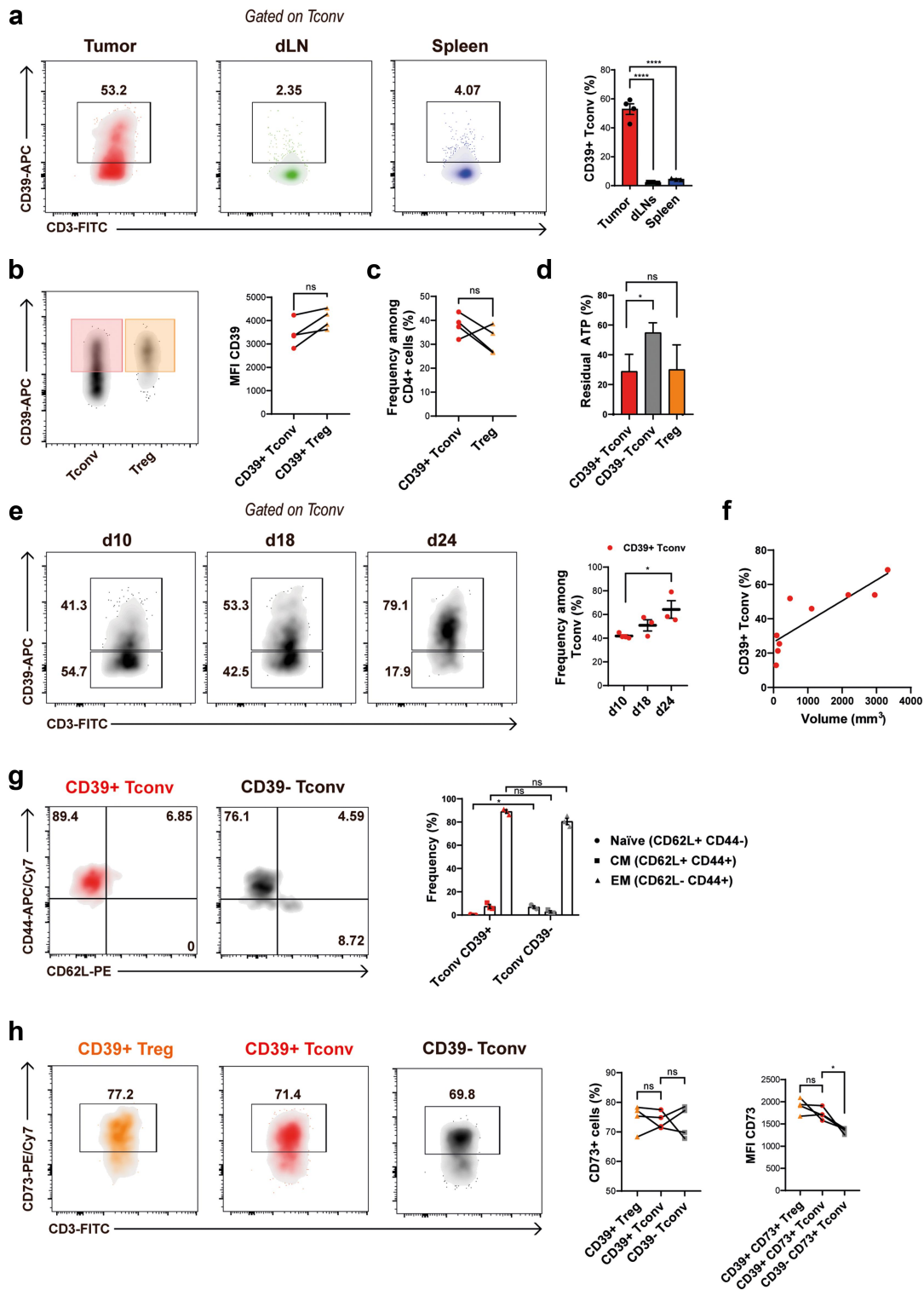
Figure 1. CD39$^+$ Tconv infiltrate tumors from B16F10-OVA tumor-bearing mice. Notes: a Representative density plots and graphs show frequency of CD39$^+$ cells gated on Tconv cells (CD4$^+$FOXP3$^-$) from tumors, dLN and spleen at day 17 p.i. (for gating strategy see Supplementary Figure S1 A and B). One way ANOVA was used to compare the groups. b Representative density plot shows CD39 expression on T-I Tconv or Treg cells. Line graph shows MFI of CD39 expression on CD39$^+$ Tconv (red dots) or CD39$^+$ Treg (orange triangles). c Frequency of CD39$^+$ Tconv (red dots) and Treg (orange triangles) among T-I CD4$^+$ cells. d Bar graphs show the percentage of residual ATP in a bioluminescent assay of exogenous ATP hydrolysis. The percentage of residual ATP was calculated as described previously.[19] e Frequency of CD39$^+$ cells gated on T-I Tconv at different time points during tumor progression. Mean values and statistical analyses (day 10 vs. day 24) are shown. One way ANOVA was used to compare the groups. f Correlation between the frequency of T-I CD39$^+$ Tconv cells and tumor volume (mm^3) from B16-OVA tumor-bearing mice. The black line represents the adjusted curve derived from a linear regression model (R^2 = 0.72). Tumor volume: V= (smallest diameter (d)^2 x largest diameter (D)) x 0.5. g Representative density plots and graphs show the frequency of cells expressing CD44 and CD62L within CD39$^+$ or CD39$^-$ T-I Tconv cells at day 17 p.i. h Representative density plots and line graphs show frequency of CD73-expressing Treg, CD39$^+$ or CD39$^-$ T-I Tconv cells at day 17 p.i. (Left panel). Line graph shows MFI of CD73 expression within CD39$^+$CD73$^+$ Treg, (orange triangles), CD39$^+$CD73$^+$ Tconv (red dots) and CD39$^-$CD73$^+$ Tconv (gray squares) (Right panel). All results are representative of 3 to 5 independent experiments. b, c, d, f, g, h Paired T test was used to compare indicated groups. a, c, d, f: data presented as mean ± SEM. ns, non-significant; * $p \leq 0.05$; ** $p \leq 0.01$; or **** $p \leq 0.0001$. b, c, h Lines indicate that data are paired.

Altogether these results suggest that CD39+ Tconv cells have the necessary arsenal involved in the adenosine production.

CD39+ Tconv shows both a cytotoxic and exhaustion transcriptomic signature

To compare the transcriptional landscape between different CD39-expressing CD4+ T-cells (Tconv and Treg) and to understand the phenotypic differences between CD39+ vs CD39− Tconv, we isolated three replicates of T-I CD4+ T cell subsets.

Using Foxp3-EGFP tumor-bearing mice we obtained CD4+GFP+ (Treg), CD4+CD39−GFP− (CD39− Tconv), and CD4+CD39+GFP− (CD39+ Tconv) from tumors by cell sorting (Figure 2a). Multidimensional scaling (MDS) demonstrated three CD4+ T cell separated subsets, indicative of their different transcriptional profiles (Figure 2b). To define the molecular profile of CD39+ Tconv, we searched for the genes differentially expressed (DEGs) between CD39+ Tconv and CD39− Tconv cells and determined that 449 and 153 genes were significantly up- or downregulated, respectively (Figure 2c). Those upregulated in CD39+ Tconv included genes associated with cytotoxicity (such as *Gzmb, Gzmc, Gzmf, Prf1, Nkg7, Eomes)*, and with T cell exhaustion (such as *Lag3, Havcr2 (*Tim-3*), Tigit, Cd160, Pdcd1 (*PD-1) and *Tox*) (Figure 2c). CD39+ Tconv also upregulated genes corresponding to chemokines (such as *Cxcl1, Ccl3, Ccl4 and Ccl5*), or genes characteristic of tissue-resident T cells (such as *Itga1 (*CD49a*), Cxcr6 and Alox5ap*), among others (see Supplementary Table S3). CD39+ Tconv displayed a reduced expression of *Tcf7* (Tcf-1) (Figure 2c), a common feature of terminally differentiated exhausted T cells that contrasts with Tcf-1 expression in cells with stem cell-like properties akin to memory T cell populations.[26]

Biological pathways enriched in CD39+ Tconv included: "positive regulation of T cell activation", "lymphocyte chemotaxis", "positive regulation of interferonγ production", "chemokine-mediated signaling pathway", as well as pathways and processes associated with NK activation, such as "cytolysis", "regulation of NK activation", "positive regulation of NK cell mediated cytotoxicity", and "positive regulation of NK cell chemotaxis" (Figure 2d). Compared to CD39− Tconv, CD39+ Tconv showed higher expression of genes related to cytotoxicity (*Flg2, Gzms, Lyz2* and *Prf1*) and T-cell exhaustion (such as iRs, *Tox, Eomes* and *Mki67*) (Figure 2e). Gene set enrichment analysis (GSEA) indicated that the transcriptional signature of CD39+ Tconv was enriched in genes associated with NK-signature and CD8+ T cell exhaustion compared to CD39− Tconv cells (Figure 2f). Overall, the transcriptional analysis revealed that T-I CD39+ Tconv from B16F10-OVA tumor-bearing mice are enriched in genes associated with T cell activation, cytotoxicity, and exhaustion compared to CD39− Tconv cells.

Since the expression of CD39 and CD73 suggests a regulatory role in CD39+ Tconv, we compared T-I CD39+ Tconv and Treg transcriptomes. Differential expression analysis highlighted that 244 genes were significantly upregulated and 203 genes significantly downregulated in CD39+ Tconv compared to Treg. As expected, CD39+ Tconv exhibited lower levels of genes typically associated with Treg, such as *Foxp3, Il10, Ctla4, Il2ra,* and *Ccr8*, among others (see Supplementary Fig. S3A and Supplementary Table S4). Notably, compared to Treg, CD39+ Tconv upregulated cytotoxicity-related genes, such as *Gzmd, Gzme, Gzmf, Crtam, Serpinb9*, and *Prf1* (Supplementary Fig. S3A). Additionally, CD39+ Tconv showed enrichment in pathways associated with lymphocyte activation, cell killing, cytolysis, and regulation of natural killer cell activation, among others (Fig. Supplementary S3B).

The phenotype of tumor-infiltrating CD39+ Tconv is associated with exhaustion and cytotoxic potential

We next evaluated the protein expression of iRs and TFs associated with T cell activation and exhaustion in T-I Tconv cells from B16F10-OVA tumor-bearing mice. Compared with their CD39− Tconv counterparts, T-I CD39+ Tconv population exhibited the highest frequency of cells expressing all the evaluated iRs (PD-1, TIGIT, Tim-3, LAG-3, and 2B4) (Figure 3a, Left panel). CD39+ Tconv exhibited higher MFI of PD-1, TIGIT, Tim-3, LAG-3, 2B4, CTLA-4, and PD-L1 than CD39− Tconv (Supplementary Fig. S4A and B). They also showed a higher proportion of iR co-expression, with a higher frequency of T cells expressing 4 or 5 iRs (Figure 3a, Right panel). Moreover, T-I CD39+ Tconv exhibited higher expression, determined as MFI, of TFs, such as T-bet, Helios, Eomes, Blimp-1, cMaf, Tox, and Ki67, but lower expression of TCF-1 than CD39− Tconv (Figure 3b). Overall, matching the transcriptional data, the protein expression of CD39 is paralleled by high expression of iRs and TFs associated with effector function and exhaustion, as well as lower TCF-1 expression.

To further evaluate CD39+ Tconv effector functions, we evaluated by FACS the frequency of cytokine production within the Tconv population. CD39+ as well as CD39− Tconv were able to produce IFNγ. Surprisingly, although CD39+ Tconv exhibited a higher percentage of IFNγ+ cells, their TNF production was lower than CD39− Tconv (Figure 3c). Furthermore, in accordance with their IFNγ production phenotype and T-bet expression, CD39+ Tconv exhibited higher cytotoxic potential than CD39− counterpart, as attested by intracellular granzyme B and perforin expression together with the CD107a mobilization after *ex vivo* stimulation (Figure 3d). These results indicate that CD39+ Tconv may have effector functions.

We next evaluated T-I OVA-specific Tconv cells from B16F10-OVA tumor-bearing mice, and we found that around 55% of OVA-specific Tconv expressed CD39+ (Figure 3e).

It has been demonstrated that the adhesion molecules CD11a and CD49d increase their expression on T lymphocytes that have been activated through the TCR.[27] Thus, analyzing the expression of CD11a and CD49d within T-I Tconv, we found a higher frequency of CD11a+CD49d+ cells within CD39+ Tconv compared to CD39− Tconv cells (Supplementary Fig. S4 C). This finding suggests that CD39+ Tconv may be enriched in tumor antigen-specific cells, including those recognizing OVA.
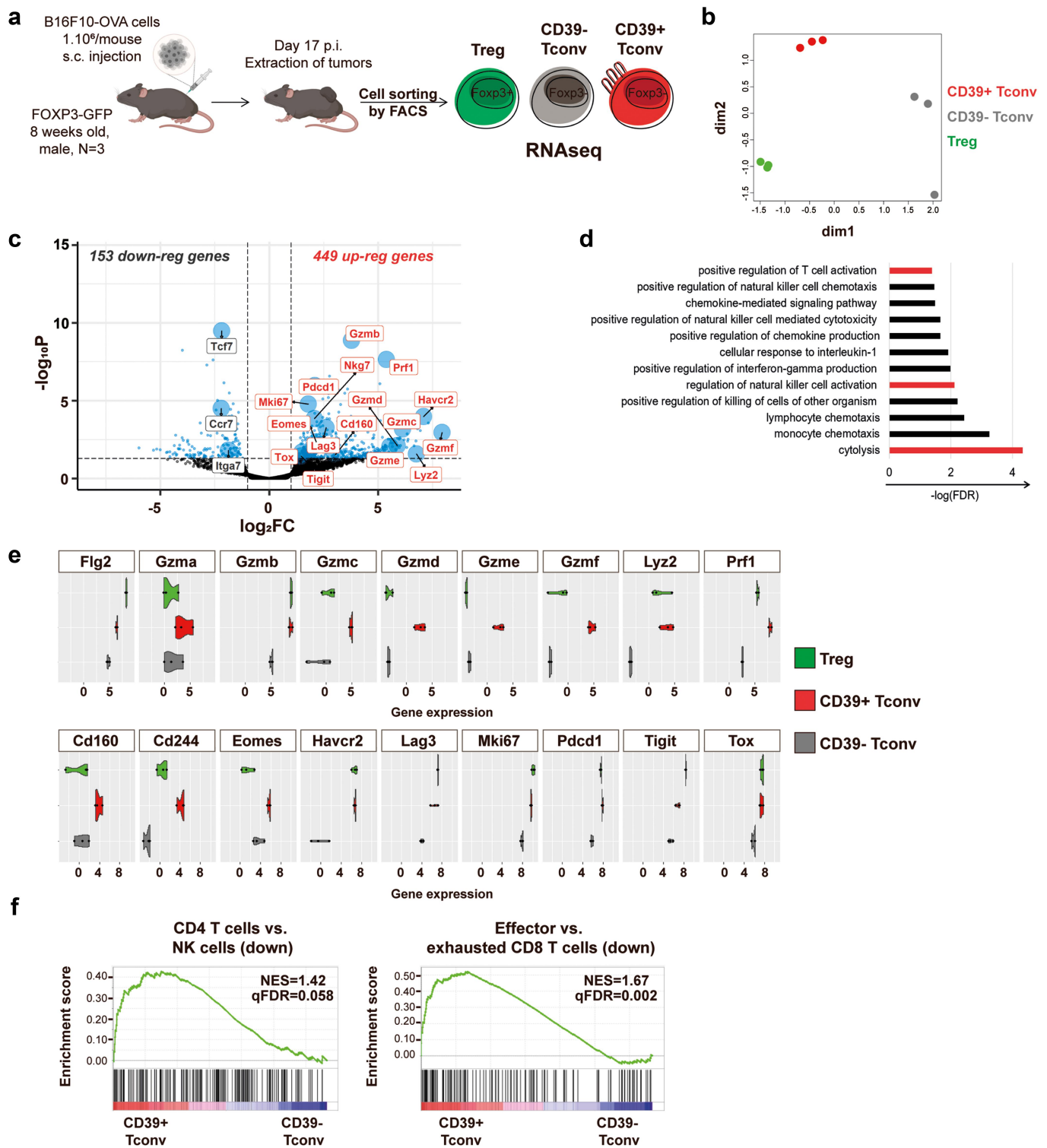
Figure 2. Transcriptional profiling of tumor-infiltrating Tconv cells. Notes: a Scheme of sort strategy for B16F10-OVA T-I Tconv and Treg cell isolation for transcriptional analysis from FOXP3-EGFP mice (N = 3). b Multidimensional scaling (MDS) two-dimensional (dim1 and dim2) scatterplot, where distances on the plot approximate the typical log2 fold changes between all the analyzed samples. Each dot represents a sample, colored by subset. c Volcano plot showing differentially expressed genes (DEGs) between CD39$^+$ Tconv and CD39$^-$ Tconv cells. Genes were considered differentially expressed if FC ≥ 2 and adjusted p value < 0.05, and these are colored in blue. Most relevant up- and downregulated genes are shown in red and gray, respectively, and are highlighted with their gene symbols. d Graph shows selected pathways significantly enriched (p < 0.05) corresponding to genes upregulated in CD39$^+$ Tconv compared to CD39$^-$ Tconv cells using the Panther Classification System. Relevant pathways are colored in red. e Violin plots show the gene expression values (voom normalized log-cpm values in log2 scale) related to cytotoxicity and T cell exhaustion on Treg (green), CD39$^+$ Tconv (red), and CD39$^-$ Tconv (gray). f GSEA plots show selected gene sets (GSE27786-left- and GSE9650-right-) enriched in CD39$^+$ Tconv vs CD39$^-$ Tconv cells. Normalized enrichment score (NES) and q False Discovery Rate (qFDR) are indicated in the graph. *p ≤0.05. P values were calculated using paired T test.
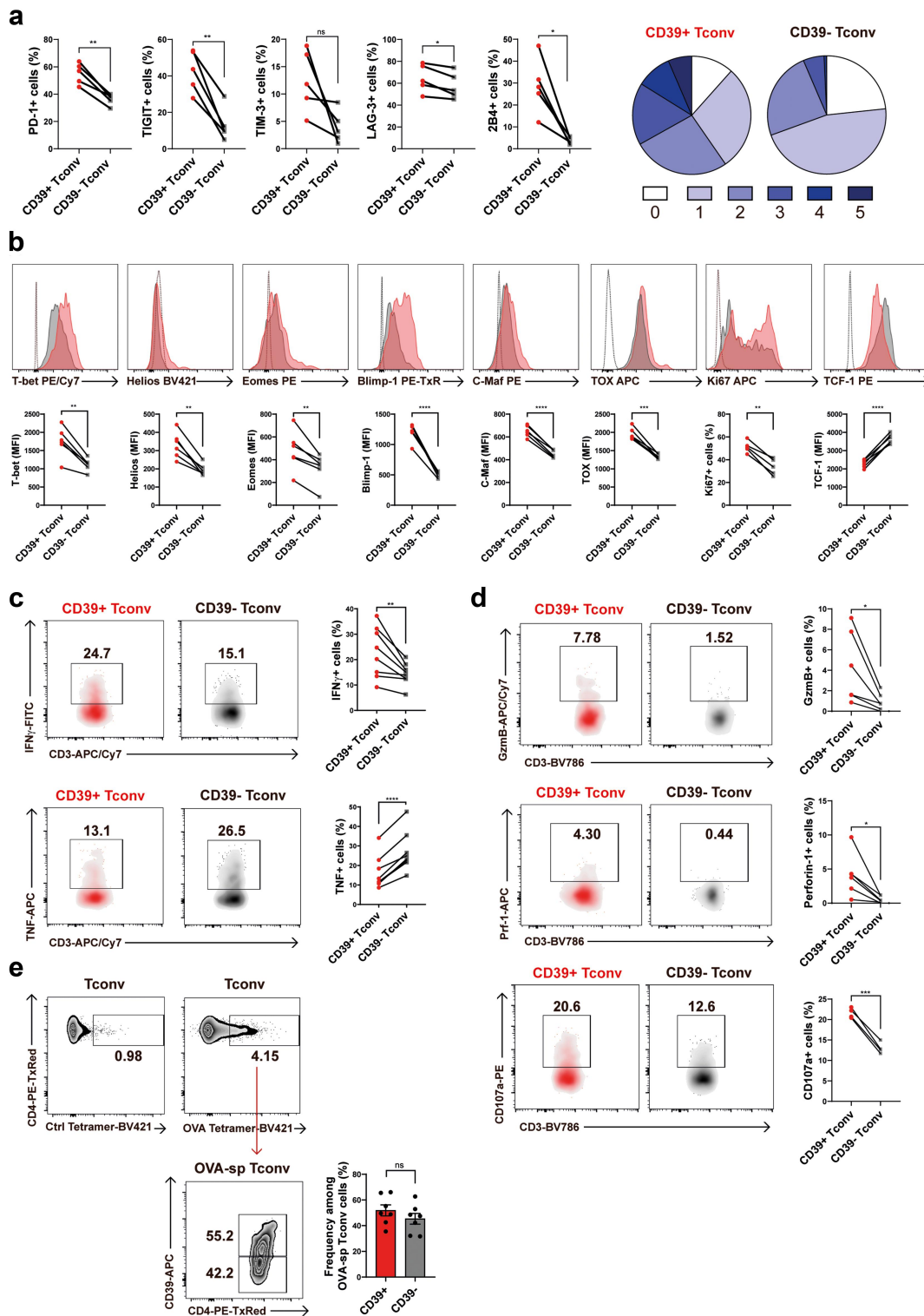
Figure 3. T-I CD39^{+} Tconv cells exhibit a phenotype of exhaustion and cytotoxicity. Notes: T-I lymphocytes were obtained from tumors from B16F10-OVA tumor-bearing mice at day 17 p.i. and analyzed by flow cytometry. a (Left panel) Line graphs show frequencies of iR-expressing CD39^{+} (red dots) or CD39^{−} (gray squares) T-I Tconv cells. (Right panel) Pie charts show the mean proportion of cells expressing zero to five of the evaluated iRs (PD-1, TIGIT, TIM-3, LAG-3 and 2B4) in CD39^{+} or CD39^{−} T-I Tconv cells. b Representative histograms and line graphs show the expression of selected TFs on CD39^{+} Tconv (red histograms, red dots) and CD39^{−} Tconv (gray histograms, gray squares). Dotted lines represent unstained controls. c Representative density plots and line graphs show the frequency of IFNγ^{+} or TNF^{+} cells among CD39^{+} (red density plots, red dots) or CD39^{−} (gray density plots, gray squares) T-I Tconv cells after PMA/Ionomycin stimulation. d Representative density plots and line graphs show the frequency of granzyme B^{+}, perforin^{+}, or CD107a^{+} cells among CD39^{+} (red density plots, red dots) or CD39^{−} (gray density plots, gray squares) T-I Tconv cells after PMA/Ionomycin stimulation. All results are representative of 3 to 5 independent experiments. e Representative zebra plots show frequency of OVA-specific Tconv cells and control (staining with H2-IAb tetramer) (upper panel). Zebra plot and graph show frequency of CD39^{+} and CD39^{−} cells within OVA-specific Tconv cells (lower panel). a-e Lines indicate that data are paired. Paired T test was used to compare CD39^{+} vs CD39^{−} Tconv cells. ns: non-significant, *p ≤0.05; **p ≤0.01; ***p ≤0.001; ****p ≤0.0001
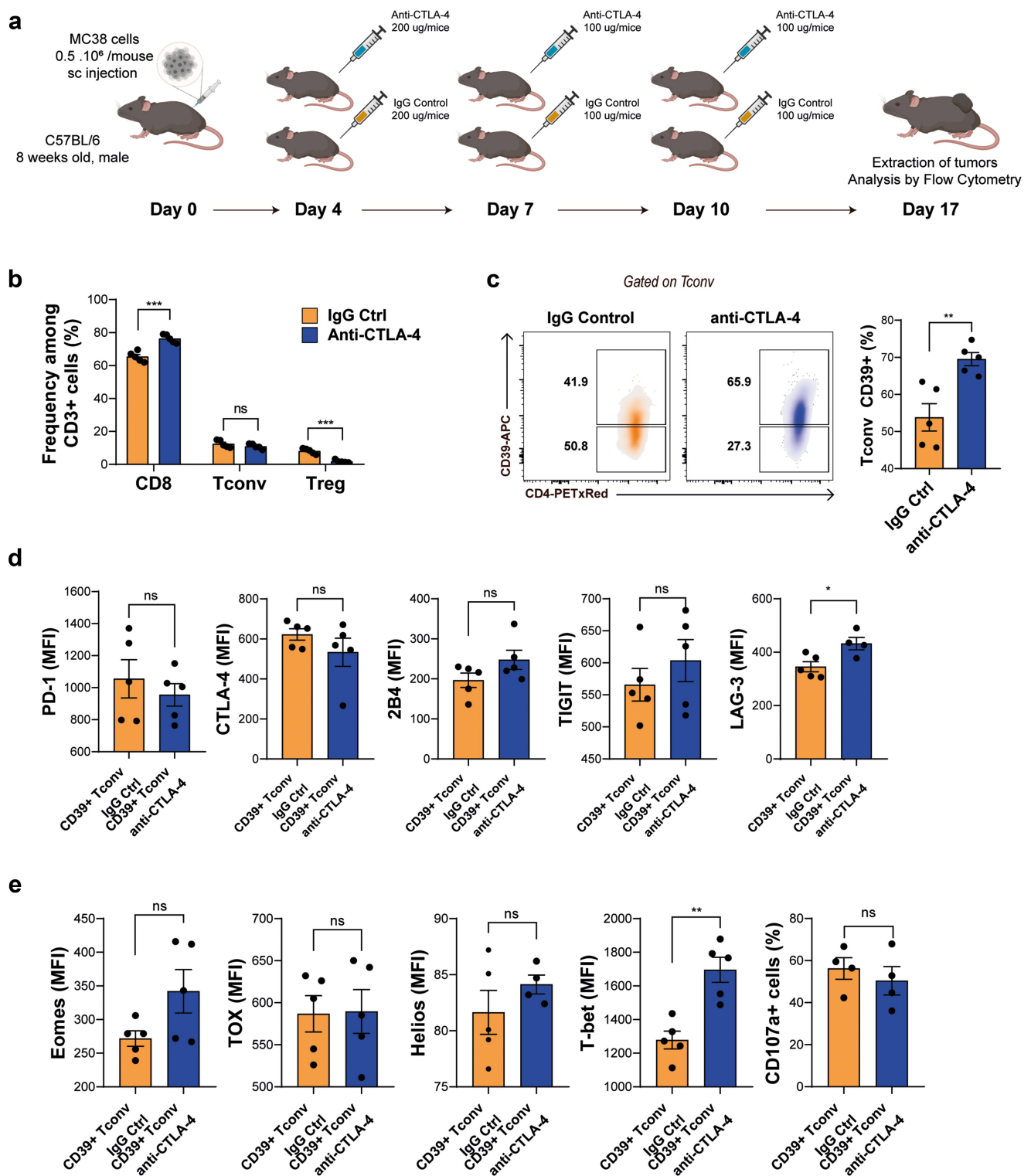
Figure 4. Anti-CTLA-4 treatment induces the expansion of T-I CD39+ Tconv cells. Notes: a Experimental design of anti-CTLA-4 treatment of MC38 tumor-bearing mice. b Graphs show frequency of T-I CD8+, Tconv and Treg cells in mice treated with anti-CTLA-4 (blue) or treated with IgG control (orange). c Representative density plots and graphs show the frequency of CD39+ Tconv cells from tumors of MC38 tumor-bearing mice treated with anti-CTLA-4 (blue) or IgG control (orange). d Bar graphs show the expression as MFI of iRs (PD-1, CTLA-4, 2B4, TIGIT, LAG-3) on T-I CD39+ Tconv cells from mice treated with anti-CTLA-4 (blue) or IgG control (orange). e Bar graphs show the expression as MFI of selected TFs (Eomes, TOX, Helios and T-bet) on T-I CD39+ Tconv from tumors of treated with anti-CTLA-4 (blue) or IgG control (orange) and frequency of CD107a+ T-I CD39+ Tconv cells from anti-CTLA-4 (blue) or IgG control (orange) treated mice. All results are representative of 2 independent experiments. b-e Data presented as mean ± SEM. *P* values were calculated using unpaired T test. ns, non-significant, *p ≤ 0.05;**p ≤ 0.01.

Overall, T-I CD39^{+} Tconv represent a distinct CD4^{+} T cell population, with transcriptomic signatures and phenotypic markers of activation/proliferation and cytotoxicity, but also exhaustion.

Anti-CTLA-4 blockade induces the expansion of T-I CD39^{+} Tconv

Anti-checkpoint blockade acts on distinct T lymphocyte subsets, with anti-PD-1 predominantly inducing the expansion of T-I exhausted CD8^{+} T cells, while anti-CTLA-4 treatment preferentially expands Th1-like CD4^{+} effector cells and reactivates exhausted CD8^{+} T cells.[28] We therefore investigated whether CTLA-4 blockade affects the T-I CD39^{+} Tconv population in mice grafted with the immunogenic MC38 colorectal tumor. Tumor-bearing mice were treated with anti-CTLA-4 or control IgG, as indicated in Figure 4a, following a previously described treatment schedule.[28] As expected, tumor growth was reduced in MC38 tumor-bearing mice with anti-CTLA-4 treatment (Supplementary Figure S5). In agreement with previous reports,[29] anti-CTLA-4 treated mice showed higher frequencies of T-I CD8^{+} T cells, reduced frequencies of Treg, and no change in Tconv frequencies among total CD3^{+} T cells, compared to IgG control-treated mice (Figure 4b). Focusing on T-I CD4^{+} T cell subpopulations, we found that anti-CTLA-4 induced an increase in CD39^{+} Tconv frequencies (Figure 4c). Notably, the expression by these expanded CD39^{+} Tconv cells of all the iRs evaluated except LAG-3 (Figure 4d), as well as of TFs related to exhaustion (Eomes, TOX, Helios), was unchanged with respect to CD39^{+} Tconv from IgG-treated mice. Furthermore, the T-I CD39^{+} Tconv subset from anti-checkpoint treated mice showed increased frequencies of cells expressing T-bet and conserved frequencies of cells able to mobilize CD107a, compared to control mice (Figure 4e).

These results indicate that anti-CTLA-4 treatment induces the expansion of T-I CD39^{+} Tconv which, despite maintaining exhaustion features, conserve their cytotoxic potential.

CD39^{+} Tconv cells accumulate within tumors and metastatic lymph nodes from breast cancer patients

Understanding the role of T-I CD4^{+} T cells in cancer patients may be key for prognosis evaluation and for the improvement of therapy design.[30] We therefore evaluated the distribution of the CD4^{+} T cell population (Treg and Tconv) in samples from 12 primary BC tumors matched with juxtatumoral breast tissue. As previously described,[31] BC tumors had a higher Treg infiltration than juxtatumoral tissues, and here we observed that the relative percentage of Tconv was significantly lower in the tumor niche than in juxtatumoral tissue (Figure 5a left panel). Nevertheless, Tconv was still the major CD4^{+} subset in both tissues. Among total Tconv, CD39^{+} cells were present at a sizable frequency both in tumoral and juxtatumoral tissues (6.07 ± 3.70% and 4.32 ± 4.12%, respectively), although the percentage was higher in tumors (Figure 5a right panel). No CD73 expression was detected in T-I CD39^{+} Tconv (data not shown). These results suggest that the TME may promote the accumulation of Treg and Tconv expressing CD39.

Considering that tumor-specific cells may be primed in the dLNs and more importantly in metastatic dLNs (M-dLNs) where tumor antigens are highly abundant, we evaluated the presence of CD39^{+} Tconv cells in metastatic and non-metastatic dLNs and peripheral blood (PB) from BC patients. In agreement with our observations regarding T-I CD8^{+} T cells,[15] M-dLNs had higher frequencies of CD39^{+} Tconv cells among total CD3^{+} cells than non-metastatic draining lymph nodes (NM-dLNs). In addition, CD39^{+} Tconv cells were not detectable in PB (Figure 5b).

We further evaluated the differential distribution of iRs in patient-matched CD39^{+} or CD39^{−} T-I Tconv cells. CD39^{+} Tconv showed significantly higher frequencies of PD-1, TIGIT and BTLA-expressing cells (Figure 5c Left panel), as well as more frequency of cells co-expressing two or three iRs (Figure 5c Right panel). Similarly, CD39^{+} Tconv cells from M-dLNs showed higher frequency of PD-1, TIGIT and BTLA-expressing cells than CD39^{−} Tconv (Supplementary Fig. S6A).

To define the phenotype of CD39^{+} Tconv in the tumor, we applied high-dimensional flow cytometry analysis to our data. Unsupervised analysis employing the dimension reduction algorithm, Uniform Manifold Approximation and Projection (UMAP), followed by the Phenograph clustering algorithm, identified 14 clusters (Figure 5d). Three clusters corresponded to Treg cells, as indicated by the expression of Foxp3^{+}, and a vast majority of these expressed CD39. Among the Tconv clusters (Foxp3^{−}), two expressed CD39, one of which showed high expression of hallmarks of exhaustion, such as TIM-3, TIGIT, BTLA, CTLA-4, and PD-1 (Tconv CD39+iRs+), while the other barely expressed CTLA-4 or TIM-3 and was negative for TIGIT, BTLA and PD-1 expression (Tconv CD39+iRs-). Considering that Tconv expressing high levels of iRs and CD39 have been associated with ongoing activation due to chronic antigen exposure at the tumor site[8], the heterogeneity within the CD39^{+} T conv may reflect different states of T cell activation.

To characterize the effector ability of human CD39^{+} Tconv cells from tumors and M-dLNs, we evaluated the frequency of TNF, IFNγ and IL-2-producing Tconv upon stimulation. We compared the frequency of cytokine-producing cells between CD39^{−} and CD39^{+} Tconv cells, focusing on non-naïve cells (gating out CD45RA^{+}CD27^{+} cells). CD39^{+} Tconv cells from tumors exhibited equal frequencies of IL-2, TNF and IFNγ producing cells, compared to CD39^{−} Tconv cells (Figure 5e). Also, CD39^{+} Tconv cells from M-dLNs showed conserved production of effector cytokines (Supplementary Fig. S6B). Notably, CD39^{+} Tconv cells from tumors exhibited higher frequencies of CD107a^{+} cells than their CD39^{−} counterparts (Figure 5e and Supplementary Fig. S6B).

Altogether, these results indicate that CD39^{+} Tconv cells present in tumors and M-dLNs from BC patients constitute a heterogeneous cell population enriched in activated cells which, although presenting some exhaustion features, are functional and conserve their cytotoxic potential even under the influence of the TME. Thus, CD39^{+} Tconv cells may emerge as key players in anti-tumor immunity.

Figure 5. CD39$^+$ Tconv cells infiltrate human breast tumors and metastatic lymph nodes and exhibit high expression of iRs. Notes: a (Left panel) Representative dot plots and line graph show frequencies of Tconv cells from tumors (violet density plot and dots) and juxtatumoral tissues (yellow density plot and dots) from BC patients (N = 13). (Right panel) Representative dot plots and line graph show frequencies of CD39$^+$ cells gated on Tconv from tumors (violet density plot and dots) and juxtatumoral tissues (yellow density plot and dots) from BC patients (N = 13). b (Left panel) Representative dot plots and line graph show frequencies of CD39$^+$ Tconv cells from matched M-dLNs (blue density plot and dots) and NM-dLNs (dark blue density plot and dots) from BC patients (N = 9). (Right panel) Representative dot plot shows frequency of CD39$^+$ Tconv cells in PB from BC patients (one out of seven samples) (gating strategies are showed in Supplementary Figure S1). c (Left panel) Line graphs show frequencies of iR-expressing CD39$^+$ (red dots) or CD39$^-$ (gray squares) T-I Tconv cells from BC patients. (Right panel) Pie charts show the mean proportion of cells expressing zero to 3 of the evaluated iRs (PD-1, TIGIT and BTLA) in CD39$^+$ or CD39$^-$ T-I Tconv cells. d (Left panel) UMAP projection of 51.100 T-I CD4$^+$ cells from BC patients (N = 7). Colors represent different clusters within CD4$^+$ cells defined by common phenotypic markers (CD45RA, CD39, CD27, FOXP3, TIM-3, TIGIT, BTLA, CTLA-4, PD-1, LAG-3). (Middle panel) UMAP projections show cells colored according to the expression of different markers: positive for FOXP3, CD39, CTLA-4, PD-1, TIGIT, and BTLA in red, and negative for those in gray. (Right panel) Heat map shows normalized expression of iRs related to exhaustion from 2 clusters highlighted as *Tconv CD39 +iRs+* and *Tconv CD39+iRslow/-*. e Representative dot plots and line graphs show frequencies of cytokine-producing cells (IL-2, TNF and IFNγ) and CD107a$^+$ cells in CD39$^+$ (red density plots and dots) and CD39$^-$ (gray density plots and squares) T-I Tconv cells from BC patients after PMA/Ionomycin stimulation (*N*=7). a, b, c, e Lines indicate that data are paired. *P* values were calculated using Wilcoxon matched-pairs signed rank test. *p ≤ 0.05, **p ≤ 0.01, *** p ≤ 0.001, ns: non-significant.

scRnaseq data reveals that CD4-CXCL13 clusters express CD39, iRs and cytolytic markers

To expand our results to other cancers beyond BC, we analyzed available single cell RNA-Seq data of CD4^{+} T cells isolated from tumors of patients with hepatocellular carcinoma (HCC),[32] colorectal cancer (CRC),[33] and non-small cell lung cancer (NSCLC).[34] We found that in CRC, CD39 was expressed in two different clusters of CD4^{+} cells (CD4_C08-IL23R and CD4_C09-CXCL13) besides the three Treg clusters (CD4_C010-FOXP3, CD4_C011-IL10, CD4_C012-CTLA4) (Figure 6a). Notably, the CD4-CXCL13 cluster concomitantly exhibited high expression of exhaustion markers (PD-1, TIGIT, TIM-3, TOX, CTLA4, and BTL-A) and cytotoxic molecules (GZMA, PRF1, and GZMB) (Figure 6b and Supplementary Fig. S7). Furthermore, co-expression of CD39 and iRs was also found in the CD4-CXCL13 cluster in HCC (Figure 6c, d, and Supplementary Fig. S7). In contrast, CD39 was expressed only in the Treg cluster of NSCLC samples (Figure 6e). Expression of CXCL13 has been previously associated with a tumor neoantigen-specific Tconv subset that can be subdivided into two clusters, one expressing memory and T follicular helper markers, and the other cytolytic markers and iRs[35]. These results and reported data reinforce the idea that CD39 may be a marker of tumor-specific CD4^{+} T cells.

High expression of CD4 and CD39 correlates with increased survival of breast cancer and melanoma patients

To explore the possible contribution of the CD39^{+} Tconv cell subset in the clinical prognosis of BC, melanoma (SKCM), hepatic cancer (LIHC), colon cancer (COAD), rectal cancer (READ), and lung cancer (LUAD), we studied overall survival in a cohort of patients from the TCGA consortium. Samples with high PTPRC (CD45) expression, high CD4 expression, and low FOXP3 expression were selected for analysis. Overall survival was calculated in the selected cohorts, stratifying patients according high or low ENTPD1 (CD39) expression. High gene expression of CD4 and ENTPD1 (CD39) correlated with a better survival of BC (Figure 7a) and melanoma (Figure 7b) patients. However, there were no significant differences in the survival of patients with LIHC, COAD, READ and LUAD (Supplementary Fig. S8). This suggests that, in some types of cancer, an expression signature including high CD4 and CD39, is associated with improved overall survival. It is plausible that, in certain forms of human cancers, other cell populations with potential pro-tumorigenic properties may also influence the patients' long-term survival outcomes.

Discussion

Antitumor CD4^{+} T cell immunity has emerged as an attractive new target in recent years.[9] Our work demonstrates that a significant frequency of T-I Tconv cells express CD39 in different experimental models. Previously, CD39 has been mostly associated with Treg and used as a marker of this cell subset[37]. Here, we show that another subset of CD4^{+} T cells expressing CD39 comprises a cell population with exhaustion and cytotoxic features. CD39^{+} Tconv cells are present in tumors and M-dLN from BC patients, but appear at lower frequencies or are even absent in PB and NM-dLNs. Their frequency is also higher in tumor than in juxtatumoral breast tissue. These observations emphasize the idea that, in mice and humans, the TME dictates CD39 expression. These results agree with those showing that CD39 expression was significantly elevated in T-I Tconv with respect to circulating CD4^{+} T cells from head and neck squamous cell carcinoma (HNSCC), lung, and colorectal cancer patients.[8,38] Similarly, it has been demonstrated that the fraction of CD4^{+} T cells expressing CD39 was also significantly higher in tumor than in healthy lung tissue from NSCLC patients.[39]

The transcriptional profile as well as flow cytometry analysis demonstrated that T-I CD39^{+} Tconv, like its CD39^{−} counterpart, from tumor-bearing mice exhibited an effector memory phenotype, but CD39^{+} Tconv cells expressed multiple iRs. These same iRs have been shown upregulated also in Tconv cells during chronic infections and cancer, and are expressed by exhausted CD8^{+} T cells, suggesting similarities between CD4^{+} and CD8^{+} T cell-exhaustion phenotypes.[17,30] Additionally, we found that its cytotoxic potential and capacity to produce IFNγ are another important feature of CD39^{+} Tconv. These findings match observations that not all effector functions of CD4^{+} exhausted T cells are necessarily compromised during chronic infection. Thus, perforin and granzyme B production in CD4^{+} T cells was higher in patients infected with HIV than in healthy controls.[40] Interestingly, such maintenance of cytotoxic functions has also been described for terminally exhausted CD8^{+} T cells.[41]

Heterogeneity is a hallmark of T cell exhaustion.[14] For CD8^{+} T cells, the transcriptional and regulatory program has been well defined.[42] However, the TFs guiding exhaustion of T-I CD4^{+} T cells are not yet well identified.[30] Indeed, different subsets within the exhausted CD4^{+} T cell population remain ill defined. Here, we observed that, compared to CD39^{−} Tconv, CD39-expressing Tconv cells display higher expression of TOX, T-bet, Eomes, Blimp-1 and cMaf, all associated with the acquisition and maintenance of effector functions and progression toward exhaustion.[14] In addition, concerning TCF-1, a TF associated with a naïve and/or stem-like phenotype, we detected the downregulation of the *Tcf7* transcript as well as lower expression of TCF-1 in CD39^{+} Tconv compared to its CD39^{−} counterpart. Recent studies indicate that T-bet drives the conversion of TCF-1^{+} progenitor exhausted CD8^{+} T cells to TCF-1^{−} cells, promoting the re-engagement of effector functions.[42] Accordingly, we speculate that high expression of T-bet on CD39^{+} Tconv may be responsible for IFNγ production. Together, our results suggest that the exhaustion program of CD4^{+} T cells resembles that of CD8^{+} T cells.

CD39 expression has been associated with antigen-mediated TCR triggering in exhausted CD8^{+} and CD4^{+} T cells. Simoni et al.[43] have shown that tumor-specific CD8^{+} T cells from colorectal and lung tumors express CD39. In the same direction, Balanca et al.[17] investigated antigen specificity
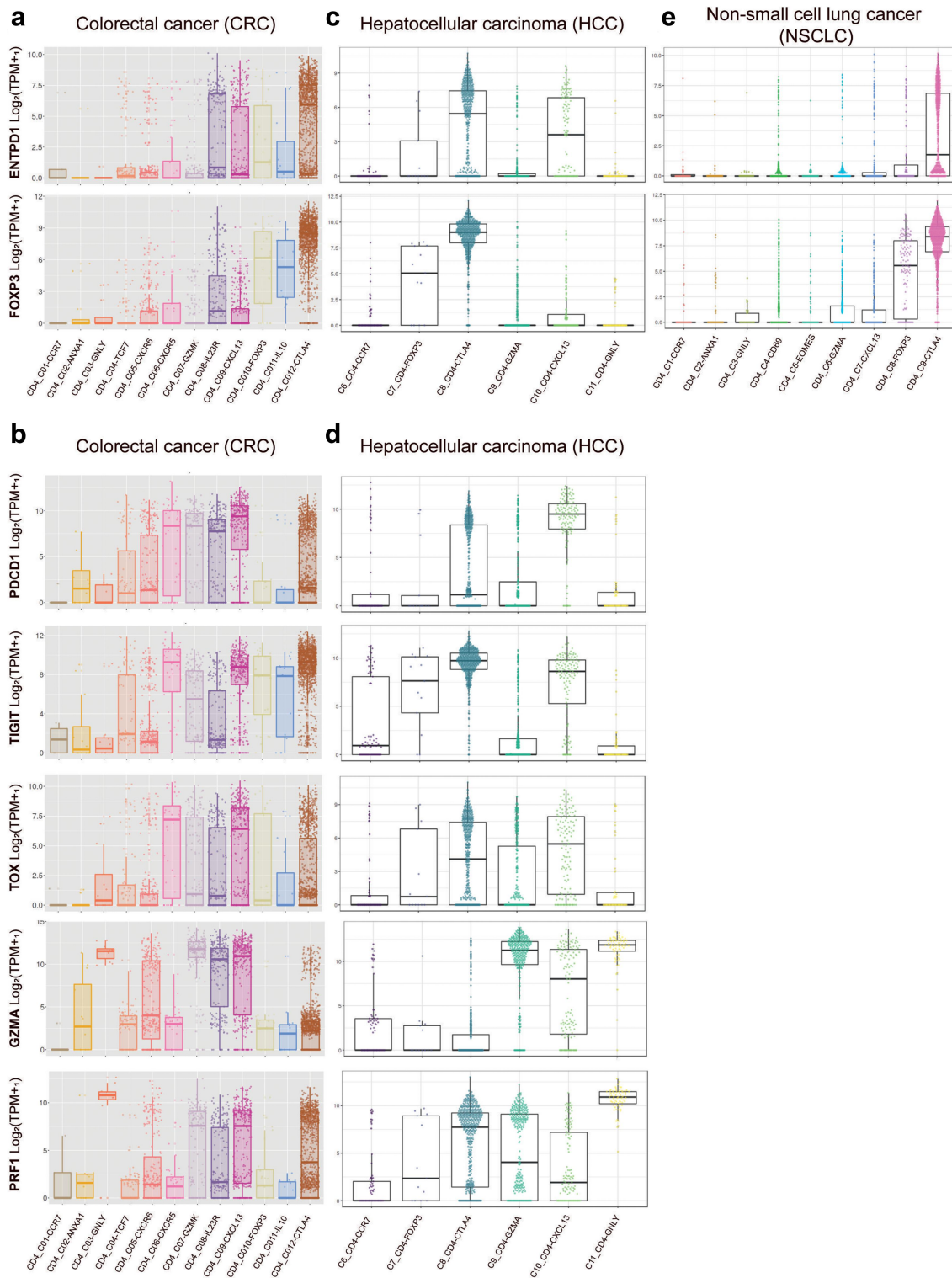
Figure 6. scRnaseq data show that CD39+ Tconv cells infiltrate tumors from HCC and CRC patients. Notes: a Analysis of ENTPD1 (CD39) and FOXP3 expression in single cells isolated from tumors of patients with colorectal cancer (CRC,[33]). b Analysis of PDCD1 (PD-1), TIGIT, TOX, GZMA and PRF1 expression in single cells isolated from tumors of patients with colorectal cancer (CRC,[33]). c Analysis of ENTPD1 (CD39) and FOXP3 expression in single cells isolated from tumors of patients with hepatocellular carcinoma (HCC,[32]). d Analysis of PDCD1 (PD-1), TIGIT, TOX, GZMA, and PRF1 expression in single cells isolated from tumors of patients with hepatocellular carcinoma (HCC,[32]). e Analysis of ENTPD1 (CD39) and FOXP3 expression in single cells isolated from tumors of patients with non-small cell lung cancer (NSCLC,[34]). Clusters are defined in the respective publications. Plots were generated through web-based platforms: http://hcc.cancer-pku.cn/forHCC; http://lung.cancer-pku.cn/forNSCLC; http://crctcell.cancer-pku.cn/forCRC.
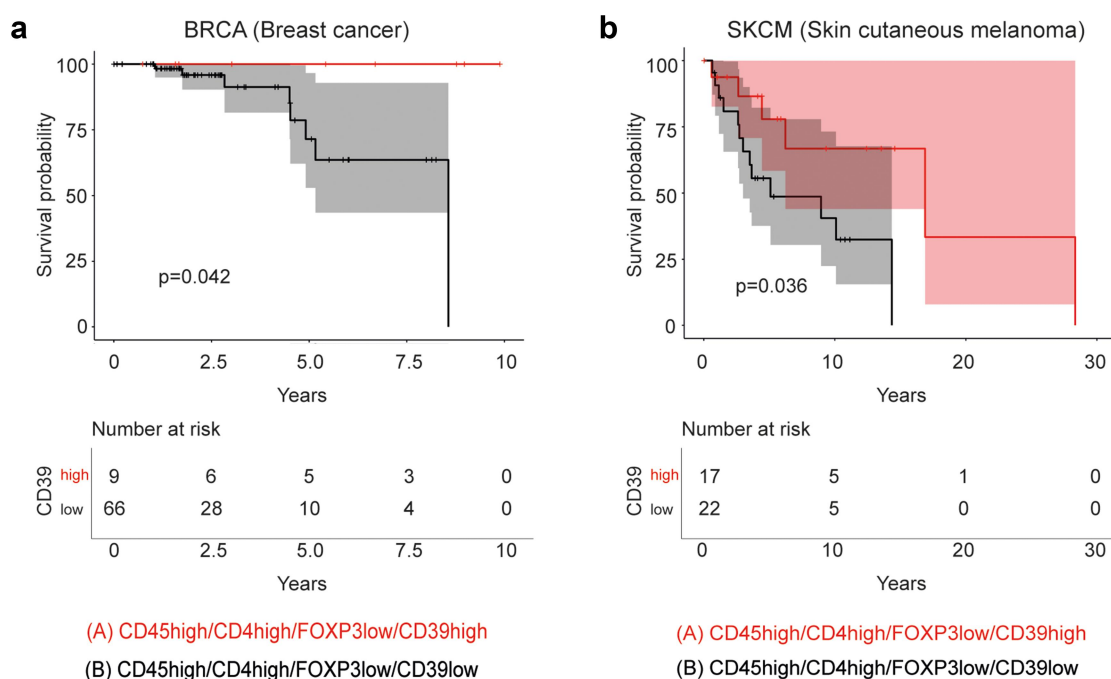
Figure 7. High expression of CD39 correlates with longer survival in patients with BC and melanoma. Notes: The overall survival (OS) of patients was calculated according to the expression level of the CD4, PTPRC (CD45), FOXP3 and ENTPD1 (CD39) genes. a, TCGA cohort of patients with BC. b; TCGA cohort of patients with melanoma. p-values of the survival analyzes were calculated with the log-rank test and are indicated in the graphs. Confidence intervals are shown in lighter shade and were calculated according to Link, C. L.[36] The number of patients at risk in function of time is shown in the tables below the survival figure.

in T-I Tconv from ovarian cancer patients, according to PD-1 and CD39 expression. While PD-1^high CD39^+ T cells were able to secrete IFNγ upon NY-ESO-1 antigen stimulation, PD-1-^high CD39^− did not respond, indicating that T-I PD-1^high CD39-^+CD4^+ encompassed tumor antigen-specific cells. More recently, Zheng et al.[32] demonstrated that neoantigen-reactive CD4^+ T cells from tumors of gastrointestinal cancer patients expressed high levels of exhaustion and cytotoxic genes. We observed that in B16F10-OVA experimental model around 55% of T-I OVA-specific Tconv cells express CD39 suggesting that at least in this murine model, CD39 cannot be used as a marker for tumor antigen-specific Tconv lymphocytes.

Here, we described that CD39^+ Tconv cells infiltrate different human tumors, where immunotherapy represents an advantageous therapeutic response, as well as in those where its efficacy has not been fully elucidated. In our study, we observed that, upon anti-CTLA-4 treatment, MC38 tumor-bearing mice exhibit a considerable expansion of CD39-expressing Tconv in addition to the expected depletion in the Treg population. After anti-CTLA-4 treatment, the expanded CD39^+ Tconv maintain the expression of molecules and TFs associated with both exhaustion and cytotoxicity, and also upregulate T-bet expression. Higher expression of this TF may prompt these cells to further produce IFNγ, contributing to an improved anti-tumor immune response, as previously reported.[44] In this line, Liakou et al.[45] demonstrated that CTLA-4 blockade increased IFNγ, producing ICOS^+CD4^+ T cells, shifting the effector to Treg cell ratio in human bladder tumors. The majority of CRC are not responsive to immune checkpoint blockage (ICB); however, it has been demonstrated that IFNγ-signaling pathways drive spontaneous

and ICB-induced antitumor immunity.[46]

PD-1 blockade influences T-I CD4^+ and CD8^+ T cells. ScRNAseq analysis of NSCLC patients' peripheral T cells pre- and post-PD-1 blockade revealed a rise in the frequency of cells in the CD4^+ effector cluster after treatment. Notably, tumor-related CD4^+ T cell clones displayed greater cytotoxic activity than CD8^+ T cell clones, highlighting the important role of tumor-related CD4^+ clones in the anti-tumor response.[47]

Hormone receptor positive or triple negative breast cancer (TNBC) patients treated with anti-PD-1 before surgery exhibited an expansion of CD8^+ and CD4^+ T cells irrespective of the tumor subtype. The expanded CD4^+ T cells were characterized by the expression of Th1 and follicular helper markers. The analysis of DEGs revealed that the expanded CD4^+ T cells exhibit markers of effector function (IFNG), cytotoxicity (GZMB, PRF1, GZMA), and exhaustion (TOX, TIGIT, PDCD1, LAG3).[48] Further studies demonstrated that TNBC patients treated with paclitaxel in combination with anti-PD-1 showed an expansion of CXCL13^+ T cells (CD4^+ and CD8^+) that expressed T cell exhaustion related genes. The expansion of CXCL13^+ T cells correlated with successful response to combination therapy.[33]

Our analysis of tumor tissue sequencing data from TGCA shows that higher expression of CD4 and CD39 transcripts in samples from BC and melanoma patients correlates with better prognosis. This observation goes in hand with the results obtained by Peter Savas et al.[49], confirming a significant association between a tissue-resident memory gene signature (i.e., iRs, CD39 and effector function associated genes) and improved survival in TNBC patients. In addition,

$CD39^+CD103^+PD-1^+CD8^+$ T-I T cells are associated with prolonged survival in patients with ovarian cancer.[50] In this regard, one limitation of our analysis is that it does not dismiss the contribution of $CD39^+$ expression in $CD8^+$ T cells. However, our previous observation that BC tumors exhibit greater proportions of T-I $CD4^+$ than $CD8^+$ T lymphocytes[20] supports the relevance of the contribution of the CD39-expressing $CD4^+$ T cell in overall survival.

Our results identify CD39 as a biomarker of Tconv cells with characteristics of exhaustion and cytotoxic potential. Uncovering the role of CD39-expressing Tconv cells in the TME should help design new strategies to improve the efficacy of current immunotherapies.

Acknowledgments

Disclosure statement

E.P. is co-founder of Egle-Tx. E.P. and J.T are consultants for Egle-Tx. The other authors declare no conflicts of interest.

Funding

Author contributions

S.B. conducted experiments, analyzed and interpreted the data, and participated in manuscript writing. C. A., J. T-B., F.P.C. and C.R, participated in experiments with mice and revised the manuscript. V.B. participated in experiments with mice. M.C.R, C.S., participated in experiments with human samples. W.R., D.R., E.F. and J.T-B. participated in biostatistics and computational analysis. A.V-S, E.B. and A.del C. provided the biological material from cancer patients. A.G. and E.V.A.R. participated in data discussion, interpretation of results and manuscript revision. C.L.M. and E.P., designed and supervised the study, analyzed and interpreted the data and wrote the manuscript.

Data availability statement

All data relevant to the study are included in the article or uploaded as supplementary information.

Sources of support

Abbreviations

BC	breast cancer
PB	peripheral blood
CTLs	cytotoxic T cells
dLNs	draining lymph nodes
iRs	inhibitory receptors
M-dLNs	metastatic draining lymph nodes
NM-dLNs	non-metastatic draining lymph nodes
OS	overall survival
Tconv	T conventional cells
TFs	transcription factors
T-I	tumor infiltrating
TME	tumor microenvironment
Treg	T regulatory cells

References

1. Borst J, Ahrends T, Babala N, Melief CJM, Kastenmüller W. CD4 (+) T cell help in cancer immunology and immunotherapy. Nat Rev Immunol. 2018;18(10):635–647. doi:10.1038/s41577-018-0044-0.

2. Hung K, Hayashi R, Lafond-Walker A, Lowenstein C, Pardoll D, Levitsky H. The central role of CD4(+) T cells in the antitumor immune response. J Exp Med. 1998;188(12):2357–2368. doi:10.1084/jem.188.12.2357.

3. Sallusto F, Lanzavecchia A. Heterogeneity of CD4+ memory T cells: functional modules for tailored immunity. Eur J Immunol. 2009;39(8):2076–2082. doi:10.1002/eji.200939722.

4. Fridman WH, Pages F, Sautes-Fridman C, Galon J. The immune contexture in human tumours: impact on clinical outcome. Nat Rev Cancer. 2012;12(4):298–306. doi:10.1038/nrc3245.

5. Takeuchi A, Saito T. CD4 CTL, a cytotoxic subset of CD4(+) T cells, their differentiation and function. Front Immunol. 2017;8:194. doi:10.3389/fimmu.2017.00194.

6. Quezada SA, Simpson TR, Peggs KS, Merghoub T, Vider J, Fan X, Blasberg R, Yagita H, Muranski P, Antony PA, et al. Tumor-reactive CD4(+) T cells develop cytotoxic activity and eradicate large established melanoma after transfer into lymphopenic hosts. J Exp Med. 2010;207(3):637–650. doi:10.1084/jem.20091918.

7. Kitano S, Tsuji T, Liu C, Hirschhorn-Cymerman D, Kyi C, Mu Z, Allison JP, Gnjatic S, Yuan JD, Wolchok JD, et al. Enhancement of tumor-reactive cytotoxic CD4+ T cell responses after ipilimumab treatment in four advanced melanoma patients. Cancer Immunol Res. 2013;1(4):235–244. doi:10.1158/2326-6066.CIR-13-0068.

8. Li S, Zhuang S, Heit A, Koo S-L, Tan AC, Chow I-T, Kwok WW, Tan IB, Tan DSW, Simoni Y, et al. Bystander CD4 + T cells infiltrate human tumors and are phenotypically distinct. Oncoimmunology. 2022;11(1):2012961. doi:10.1080/2162402X.2021.2012961.

9. Poncette L, Bluhm J, Blankenstein T. The role of CD4 T cells in rejection of solid tumors. Curr Opin Immunol. 2022;74:18–24. doi:10.1016/j.coi.2021.09.005.

10. Baitsch L, Baumgaertner P, Devevre E, Raghav SK, Legat A, Barba L, Wieckowski S, Bouzourene H, Deplancke B, Romero P, et al. Exhaustion of tumor-specific CD8(+) T cells in metastases from melanoma patients. J Clin Invest. 2011;121(6):2350–2360. doi:10.1172/JCI46102.

11. Blackburn SD, Shin H, Haining WN, Zou T, Workman CJ, Polley A, Betts MR, Freeman GJ, Vignali DAA, Wherry EJ, et al. Coregulation of CD8+ T cell exhaustion by multiple inhibitory receptors during chronic viral infection. Nat Immunol. 2009;10 (1):29–37. doi:10.1038/ni.1679.

12. Wherry EJ. T cell exhaustion. Nat Immunol. 2011;12(6):492–499. doi:10.1038/ni.2035.

13. Khan O, Giles JR, McDonald S, Manne S, Ngiow SF, Patel KP, Werner MT, Huang AC, Alexander KA, Wu JE, et al. TOX transcriptionally and epigenetically programs CD8(+) T cell exhaustion. Nature. 2019;571(7764):211–218. doi:10.1038/s41586-019-1325-x.

14. McLane LM, Abdel-Hakeem MS, Wherry EJ. CD8 T cell exhaustion during chronic viral infection and cancer. Annu Rev Immunol. 2019;37(1):457–495. doi:10.1146/annurev-immunol-041015-055318.

15. Canale FP, Ramello MC, Nunez N, Furlan CLA, Bossio SN, Serrán MG, Boari JT, Del Castillo A, Ledesma M, Sedlik C, et al. CD39 expression defines cell exhaustion in tumor-infiltrating CD8 (+) T cells. Cancer Res. 2018;78(1):115–128. doi:10.1158/0008-5472.CAN-16-2684.

16. Duhen T, Duhen R, Montler R, Moses J, Moudgil T, de Miranda NF, Goodall CP, Blair TC, Fox BA, McDermott JE, et al. Co-expression of CD39 and CD103 identifies tumor-reactive CD8 T cells in human solid tumors. Nat Commun. 2018;9(1):2724. doi:10.1038/s41467-018-05072-0.

17. Balanca CC, Salvioni A, Scarlata CM, Michelas M, Martinez-Gomez C, Gomez-Roca C, Sarradin V, Tosolini M, Valle C, Pont F, et al. PD-1 blockade restores helper activity of tumor-infiltrating, exhausted PD-1hiCD39+ CD4 T cells. JCI Insight. 2021;6(2). doi:10.1172/jci.insight.142513.

18. Kortekaas KE, Santegoets SJ, Sturm G, Ehsan I, van Egmond SL, Finotello F, Trajanoski Z, Welters MJP, van Poelgeest MIE, van der Burg SH, et al. CD39 identifies the CD4(+) tumor-specific T-cell population in human cancer. Cancer Immunol Res. 2020;8 (10):1311–1321. doi:10.1158/2326-6066.CIR-20-0270.

19. Zacca ER, Amezcua Vesely MC, Ferrero PV, Acosta CDV, Ponce NE, Bossio SN, Mussano E, Onetti L, Cadile I, Acosta Rodríguez EV, et al. B cells from patients with rheumatoid arthritis show conserved CD39-mediated regulatory function and increased CD39 expression after positive response to therapy. J Mol Biol. 2021;433(1):166687. doi:10.1016/j.jmb.2020.10.021.

20. Ramello MC, Nunez NG, Tosello Boari J, Bossio SN, Canale FP, Abrate C, Ponce N, Del Castillo A, Ledesma M, Viel S, et al. Polyfunctional KLRG-1(+)CD57(+) Senescent CD4(+) T cells infiltrate tumors and are expanded in peripheral blood from breast cancer patients. Front Immunol. 2021;12:713132. doi:10.3389/fimmu.2021.713132.

21. Dobin A, Davis CA, Schlesinger F, Drenkow J, Zaleski C, Jha S, Batut P, Chaisson M, Gingeras TR. STAR: ultrafast universal RNA-seq aligner. Bioinformatics. 2013;29(1):15–21. doi:10.1093/bioinformatics/bts635.

22. Weinstein JN, Collisson EA, Mills GB, Shaw KRM, Ozenberger BA, Ellrott K, Shmulevich I, Sander C, Stuart JM. The cancer genome atlas pan-cancer analysis project. Nat Genet. 2013;45 (10):1113–1120. doi:10.1038/ng.2764.

23. Wei L, Jin Z, Yang S, Xu Y, Zhu Y, Ji Y. TCGA-assembler 2: software pipeline for retrieval and processing of TCGA/CPTAC data. Bioinformatics. 2018;34(9):1615–1617. doi:10.1093/bioinformatics/btx812.

24. Robinson MD, McCarthy DJ, Smyth GK. edgeR: a Bioconductor package for differential expression analysis of digital gene expression data. Bioinformatics. 2010;26(1):139–140. doi:10.1093/bioinformatics/btp616.

25. Alboukadel K, Marcin K, Przemyslaw B. Survminer: Drawing survival Curves using "ggplot2". 2021.

26. Blank CU, Haining WN, Held W, Hogan PG, Kallies A, Lugli E, Lynn RC, Philip M, Rao A, Restifo NP, et al. Defining 'T cell exhaustion'. Nat Rev Immunol. 2019;19(11):665–674. doi:10.1038/s41577-019-0221-9.

27. Moretto MM, Hwang S, Khan IA. Downregulated IL-21 response and T follicular helper cell exhaustion correlate with compromised CD8 T cell immunity during chronic Toxoplasmosis. Front Immunol. 2017;8:1436. doi:10.3389/fimmu.2017.01436.

28. Wei SC, Levine JH, Cogdill AP, Zhao Y, Anang NAAS, Andrews MC, Sharma P, Wang J, Wargo JA, Pe'er D, et al. Distinct cellular mechanisms underlie anti-CTLA-4 and anti-PD-1 checkpoint blockade. Cell. 2017;170(6):1120–1133.e17. doi:10.1016/j.cell.2017.07.024.

29. Willsmore ZN, Coumbe BGT, Crescioli S, Reci S, Gupta A, Harris RJ, Chenoweth A, Chauhan J, Bax HJ, McCraw A, et al. Combined anti-PD-1 and anti-CTLA-4 checkpoint blockade: Treatment of melanoma and immune mechanisms of action. Eur J Immunol. 2021;51(3):544–556. doi:10.1002/eji.202048747.

30. Miggelbrink AM, Jackson JD, Lorrey SJ, Srinivasan ES, Waibl-Polania J, Wilkinson DS, Fecci PE. CD4 T-Cell exhaustion: does it exist and what are its roles in cancer? Clin Cancer Res. 2021;27 (21):5742–5752. doi:10.1158/1078-0432.CCR-21-0206.

31. Plitas G, Konopacki C, Wu K, Bos PD, Morrow M, Putintseva E, Chudakov D, Rudensky A. Regulatory T cells exhibit distinct features in human breast cancer. Immunity. 2016;45 (5):1122–1134. doi:10.1016/j.immuni.2016.10.032.

32. Zheng C, Zheng L, Yoo JK, Guo H, Zhang Y, Guo X, Kang B, Hu R, Huang JY, Zhang Q, et al. Landscape of infiltrating T cells in Liver cancer revealed by single-cell sequencing. Cell. 2017;169(7):1342–1356.e16. doi:10.1016/j.cell.2017.05.035.

33. Zhang L, Yu X, Zheng L, Zhang Y, Li Y, Fang Q, Gao R, Kang B, Zhang Q, Huang JY, et al. Lineage tracking reveals dynamic relationships of T cells in colorectal cancer. Nature. 2018;564 (7735):268–272. doi:10.1038/s41586-018-0694-x.

34. Guo X, Zhang Y, Zheng L, Zheng C, Song J, Zhang Q, Kang B, Liu Z, Jin L, Xing R, et al. Global characterization of T cells in non-small-cell lung cancer by single-cell sequencing. Nat Med. 2018;24(7):978–985. doi:10.1038/s41591-018-0045-3.

35. Veatch JR, Lee SM, Shasha C, Singhi N, Szeto JL, Moshiri AS, Kim TS, Smythe K, Kong P, Fitzgibbon M, et al. Neoantigen-specific CD4+ T cells in human melanoma have diverse differentiation states and correlate with CD8+ T cell, macrophage, and B cell function. Cancer Cell. 2022;40(4):393–409.e9. doi:10.1016/j.ccell.2022.03.006.

36. Link CL. Confidence intervals for the survival function using Cox's proportional-hazard model with covariates. Biometrics. 1984;40 (3):601–609. doi:10.2307/2530904.

37. Deaglio S, Dwyer KM, Gao W, Friedman D, Usheva A, Erat A, Chen J-F, Enjyoji K, Linden J, Oukka M, et al. Adenosine generation catalyzed by CD39 and CD73 expressed on regulatory T cells mediates immune suppression. J Exp Med. 2007;204(6):1257–1265. doi:10.1084/jem.20062512.

38. Schuler PJ, Schilling B, Harasymczuk M, Hoffmann TK, Johnson J, Lang S, Whiteside TL. Phenotypic and functional characteristics of CD4+ CD39+ FOXP3+ and CD4+ CD39+ FOXP3neg T-cell subsets in cancer patients. Eur J Immunol. 2012;42(7):1876–1885. doi:10.1002/eji.201142347.

39. Tondell A, Wahl SGF, Sponaas AM, Sørhaug S, Børset M, Haug M. Ectonucleotidase CD39 and checkpoint signalling receptor programmed death 1 are highly elevated in intratumoral immune cells in non–small-cell lung cancer. Transl Oncol. 2020;13 (1):17–24. doi:10.1016/j.tranon.2019.09.003.

40. Salwe S, Singh A, Padwal V, Velhal S, Nagar V, Patil P, Deshpande A, Patel V. Immune signatures for HIV-1 and HIV-2 induced CD4(+)T cell dysregulation in an Indian cohort. BMC Infect Dis. 2019;19(1):135. doi:10.1186/s12879-019-3743-7.

41. Miller BC, Sen DR, Al Abosy R, Bi K, Virkud YV, LaFleur MW, Yates KB, Lako A, Felt K, Naik GS, et al. Subsets of exhausted CD8 (+) T cells differentially mediate tumor control and respond to checkpoint blockade. Nat Immunol. 2019;20(3):326–336. doi:10.1038/s41590-019-0312-6.

42. Beltra JC, Manne S, Abdel-Hakeem MS, Kurachi M, Giles JR, Chen Z, Casella V, Ngiow SF, Khan O, Huang YJ, et al. Developmental relationships of four exhausted CD8(+) T cell subsets reveals underlying transcriptional and epigenetic landscape control mechanisms. Immunity. 2020;52(5):825–841.e8. doi:10.1016/j.immuni.2020.04.014.

43. Simoni Y, Becht E, Fehlings M, Loh CY, Koo S-L, Teng KWW, Yeong JPS, Nahar R, Zhang T, Kared H, et al. Bystander CD8(+) T cells are abundant and phenotypically distinct in human tumour infiltrates. Nature. 2018;557(7706):575–579. doi:10.1038/s41586-018-0130-2.

44. Wang W, Green M, Choi JE, Gijón M, Kennedy PD, Johnson JK, Liao P, Lang X, Kryczek I, Sell A, et al. CD8(+) T cells regulate tumour ferroptosis during cancer immunotherapy. Nature. 2019;569(7755):270–274. doi:10.1038/s41586-019-1170-y.

45. Liakou CI, Kamat A, Tang DN, Chen H, Sun J, Troncoso P, Logothetis C, Sharma P. CTLA-4 blockade increases IFNγ-producing CD4 + ICOS hi cells to shift the ratio of effector to regulatory T cells in cancer patients. Proc Natl Acad Sci U S A. 2008;105(39):14987–14992. doi:10.1073/pnas.0806075105.

46. Du W, Frankel TL, Green M, Zou W. IFNγ signaling integrity in colorectal cancer immunity and immunotherapy. Cell Mol Immunol. 2022;19(1):23–32. doi:10.1038/s41423-021-00735-3.

47. Zhang F, Bai H, Gao R, Fei K, Duan J, Zhang Z, Wang J, Hu X. Dynamics of peripheral T cell clones during PD-1 blockade in non-small cell lung cancer. Cancer Immunol Immunother. 2020;69(12):2599–2611. doi:10.1007/s00262-020-02642-4.

48. Bassez A, Vos H, Van Dyck L, Floris G, Arijs I, Desmedt C, Boeckx B, Vanden Bempt M, Nevelsteen I, Lambein K, et al. A single-cell map of intratumoral changes during anti-PD1 treatment of patients with breast cancer. Nat Med. 2021;27(5):820–832. doi:10.1038/s41591-021-01323-8.

49. Savas P, Virassamy B, Ye C, Salim A, Mintoff CP, Caramia F, Salgado R, Byrne DJ, Teo ZL, Dushyanthen S, et al. Single-cell profiling of breast cancer T cells reveals a tissue-resident memory subset associated with improved prognosis. Nat Med. 2018;24 (7):986–993. doi:10.1038/s41591-018-0078-7.

50. Laumont CM, Wouters MCA, Smazynski J, Gierc NS, Chavez EA, Chong LC, Thornton S, Milne K, Webb JR, Steidl C, et al. Single-cell profiles and prognostic impact of tumor-infiltrating lympho-cytes coexpressing CD39, CD103, and PD-1 in ovarian cancer. Clin Cancer Res. 2021;27(14):4089–4100. doi:10.1158/1078-0432.CCR-20-4394.